Mfront user meeting 2022

# Damage mechanics implementations using MFront: orthotropic, anisotropic microplane and embedded strong-discontinuity models for quasi-brittle materials

**Breno Ribeiro Nogueira** [a,c]

Héloïse Rostagni [a], Giuseppe Rastiello [b], Cédric Giry [a], Fabrice Gatuingt [a], Carlo Callari [c], Frédéric Ragueneau [a], Ibrahim Bitar [d] and Benjamin Richard [d]

[a] Université Paris-Saclay, CentraleSupélec, ENS Paris-Saclay, CNRS, Laboratoire de Mécanique Paris-Saclay
[b] Université Paris-Saclay, CEA, Service d'études mécaniques et thermiques
[c] Università degli Studi del Molise, Engineering Division, DiBT, Campobasso (Italie)
[d] Institut de Radioprotection et de Sûreté Nucléaire (IRSN), PSN-EXP/SES/LMAPS, France

October 2022

# Plan



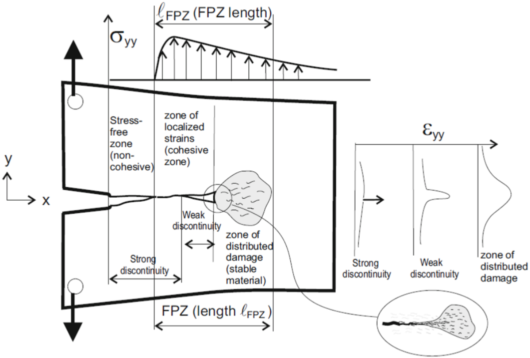


Illustrative scheme of the Fracture Process Zone (FPZ) [1]

1. Huespe and Oliver, 2011.

# Introduction

# Introduction

- **Why study crack?**
  - Usual structural design codes $\Rightarrow$ economic and primarily environmental costs
  - Special constructions (e.g., nuclear reactor, dam, historical buildings, etc.)
  - The need to provide a better comprehension of degradation mechanisms
- **Predict the cracking behavior**
  - Estimate crack opening
  - Degradation level following a specific loading scenario
- **Study frameworks**
  - Continuum damage mechanics
  - Explicit description of crack (strong discontinuities)

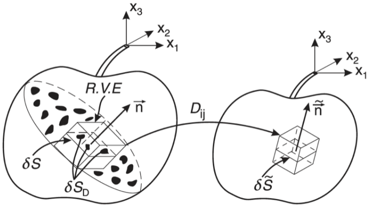


Illustrative scheme of damage volume element [2]

2. Lemaitre and Desmorat, 2005.

# Microplane models

# Basic principles

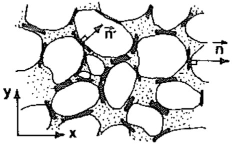


Physical justification [3]

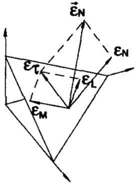


Microplane strains [4]

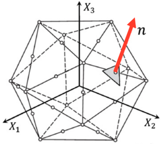


Spherical discretization [5]

1. Influenced by the theory introduced by Taylor in polycrystalline metals plasticity (Taylor, 1938)
2. Macroscopic strain tensor projected on each microplane (kinematic constraint)
3. Constitutive relations defined in a simple and practical way
4. Macroscopic stress tensor obtained by the means of the principle of virtual work
5. Microplane parameters obtained in function of macroscopic ones

3. Bažant and Gambarova, 1984.
4. Bažant et al., 1996.
5. Caner and Bažant, 2013.

# Basic principles

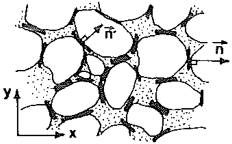

Physical justification [3]

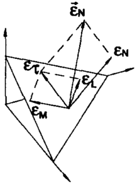
Microplane strains [4]

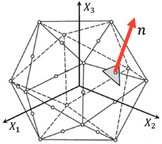

Spherical discretization [5]

1. Influenced by the theory introduced by Taylor in polycrystalline metals plasticity (Taylor, 1938)
2. Macroscopic strain tensor projected on each microplane (kinematic constraint)
3. Constitutive relations defined in a simple and practical way
4. Macroscopic stress tensor obtained by the means of the principle of virtual work
5. Microplane parameters obtained in function of macroscopic ones

3. Bažant and Gambarova, 1984.
4. Bažant et al., 1996.
5. Caner and Bažant, 2013.

# Basic principles

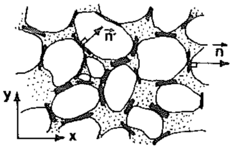


Physical justification [3]

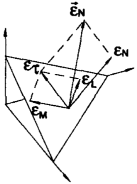


Microplane strains [4]

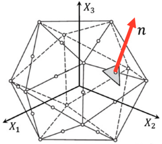


Spherical discretization [5]

1. Influenced by the theory introduced by Taylor in polycrystalline metals plasticity (Taylor, 1938)
2. Macroscopic strain tensor projected on each microplane (kinematic constraint)
3. Constitutive relations defined in a simple and practical way
4. Macroscopic stress tensor obtained by the means of the principle of virtual work
5. Microplane parameters obtained in function of macroscopic ones

3. Bažant and Gambarova, 1984.
4. Bažant et al., 1996.
5. Caner and Bažant, 2013.

# Basic principles

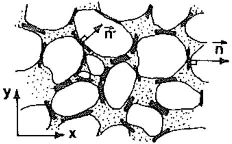


Physical justification [3]

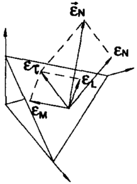


Microplane strains [4]

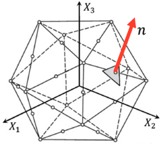


Spherical discretization [5]

3. Bažant and Gambarova, 1984.
4. Bažant et al., 1996.
5. Caner and Bažant, 2013.

1. Influenced by the theory introduced by Taylor in polycrystalline metals plasticity (Taylor, 1938)
2. Macroscopic strain tensor projected on each microplane (kinematic constraint)
3. Constitutive relations defined in a simple and practical way
4. Macroscopic stress tensor obtained by the means of the principle of virtual work
5. Microplane parameters obtained in function of macroscopic ones

# Basic principles

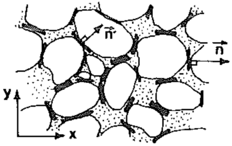


Physical justification [3]

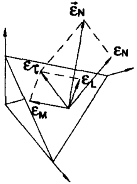


Microplane strains [4]

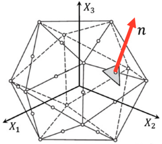


Spherical discretization [5]

1. Influenced by the theory introduced by Taylor in polycrystalline metals plasticity (Taylor, 1938)
2. Macroscopic strain tensor projected on each microplane (kinematic constraint)
3. Constitutive relations defined in a simple and practical way
4. Macroscopic stress tensor obtained by the means of the principle of virtual work
5. Microplane parameters obtained in function of macroscopic ones

---

3. Bažant and Gambarova, 1984.
4. Bažant et al., 1996.
5. Caner and Bažant, 2013.

# Disk simplification

(Kakarla et al., 2021;Kakarla, 2020; Park and Kim, 2003)

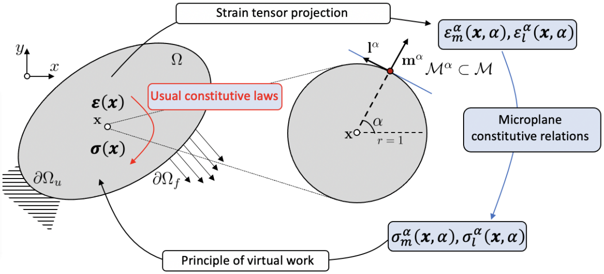


## Projection

$$\epsilon_m^\alpha = \boldsymbol{m}^\alpha \cdot \boldsymbol{\epsilon} \cdot \boldsymbol{m}^\alpha = \boldsymbol{M}^\alpha : \boldsymbol{\epsilon} = (\boldsymbol{m}^\alpha \otimes \boldsymbol{m}^\alpha) : \boldsymbol{\epsilon}$$

$$\epsilon_l^\alpha = \boldsymbol{l}^\alpha \cdot \boldsymbol{\epsilon} \cdot \boldsymbol{m}^\alpha = \boldsymbol{L}^\alpha : \boldsymbol{\epsilon} = (\boldsymbol{l}^\alpha \otimes \boldsymbol{m}^\alpha)^s : \boldsymbol{\epsilon}$$

## Principle of virtual work

$$\pi \boldsymbol{\sigma} : \delta\boldsymbol{\epsilon} = \int_{\mathcal{M}} (\sigma_m^\alpha \delta\epsilon_m^\alpha + \sigma_l^\alpha \delta\epsilon_l^\alpha) dS$$

$$\boldsymbol{\sigma} = \frac{2}{\pi} \sum_{N^\alpha} (\sigma_m^\alpha \boldsymbol{M}^\alpha + \sigma_l^\alpha \boldsymbol{L}^\alpha) W_\alpha$$

## Behaviour

$$\rho\psi^\alpha = (1-\omega^\alpha)/2 \left[E_m(\epsilon_m^\alpha)^2 + E_l(\epsilon_l^\alpha)^2\right]$$

$$\sigma_{m,l}^\alpha = \frac{\partial \rho\psi^\alpha}{\partial \epsilon_{m,l}^\alpha} = (1-\omega^\alpha) E_{m,l} \epsilon_{m,l}^\alpha$$

$$\mathbb{C}_s^\alpha = (1-\omega^\alpha)\left[E_m(\boldsymbol{M}^\alpha \otimes \boldsymbol{M}^\alpha) + E_l(\boldsymbol{L}^\alpha \otimes \boldsymbol{L}^\alpha)\right]$$

# Disk simplification

(Kakarla et al., 2021;Kakarla, 2020; Park and Kim, 2003)

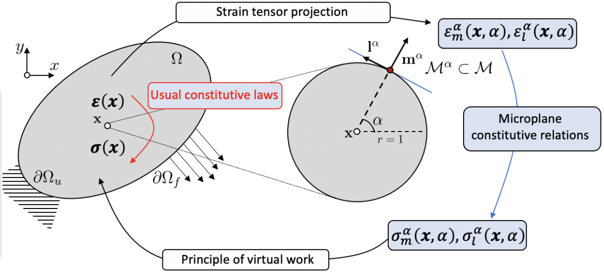


## *Projection*

$$\epsilon_m^\alpha = \boldsymbol{m}^\alpha \cdot \boldsymbol{\epsilon} \cdot \boldsymbol{m}^\alpha = \boldsymbol{M}^\alpha : \boldsymbol{\epsilon} = (\boldsymbol{m}^\alpha \otimes \boldsymbol{m}^\alpha) : \boldsymbol{\epsilon}$$

$$\epsilon_l^\alpha = \boldsymbol{l}^\alpha \cdot \boldsymbol{\epsilon} \cdot \boldsymbol{m}^\alpha = \boldsymbol{L}^\alpha : \boldsymbol{\epsilon} = (\boldsymbol{l}^\alpha \otimes \boldsymbol{m}^\alpha)^s : \boldsymbol{\epsilon}$$

## *Principle of virtual work*

$$\pi \boldsymbol{\sigma} : \delta\boldsymbol{\epsilon} = \int_{\mathcal{M}} (\sigma_m^\alpha \delta\epsilon_m^\alpha + \sigma_l^\alpha \delta\epsilon_l^\alpha) dS$$

$$\boldsymbol{\sigma} = \frac{2}{\pi} \sum_{N^\alpha} (\sigma_m^\alpha \boldsymbol{M}^\alpha + \sigma_l^\alpha \boldsymbol{L}^\alpha) W_\alpha$$

## *Behaviour*

$$\rho\psi^\alpha = (1-\omega^\alpha)/2 \left[E_m (\epsilon_m^\alpha)^2 + E_l (\epsilon_l^\alpha)^2\right]$$

$$\sigma_{m,l}^\alpha = \frac{\partial \rho\psi^\alpha}{\partial \epsilon_{m,l}^\alpha} = (1-\omega^\alpha) E_{m,l} \epsilon_{m,l}^\alpha$$

$$\mathbb{C}_s^\alpha = (1-\omega^\alpha)\left[E_m (\boldsymbol{M}^\alpha \otimes \boldsymbol{M}^\alpha) + E_l (\boldsymbol{L}^\alpha \otimes \boldsymbol{L}^\alpha)\right]$$

# Disk simplification

(Kakarla et al., 2021;Kakarla, 2020; Park and Kim, 2003)

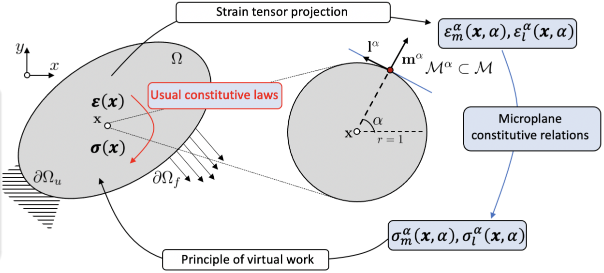


## *Projection*

$$\epsilon_m^\alpha = \boldsymbol{m}^\alpha \cdot \boldsymbol{\epsilon} \cdot \boldsymbol{m}^\alpha = \boldsymbol{M}^\alpha : \boldsymbol{\epsilon} = (\boldsymbol{m}^\alpha \otimes \boldsymbol{m}^\alpha) : \boldsymbol{\epsilon}$$

$$\epsilon_l^\alpha = \boldsymbol{l}^\alpha \cdot \boldsymbol{\epsilon} \cdot \boldsymbol{m}^\alpha = \boldsymbol{L}^\alpha : \boldsymbol{\epsilon} = (\boldsymbol{l}^\alpha \otimes \boldsymbol{m}^\alpha)^s : \boldsymbol{\epsilon}$$

## *Principle of virtual work*

$$\pi \boldsymbol{\sigma} : \delta \boldsymbol{\epsilon} = \int_{\mathcal{M}} (\sigma_m^\alpha \delta \epsilon_m^\alpha + \sigma_l^\alpha \delta \epsilon_l^\alpha) dS$$

$$\boldsymbol{\sigma} = \frac{2}{\pi} \sum_{N^\alpha} (\sigma_m^\alpha \boldsymbol{M}^\alpha + \sigma_l^\alpha \boldsymbol{L}^\alpha) W_\alpha$$

## *Behaviour*

$$\rho\psi^\alpha = (1-\omega^\alpha)/2 \left[E_m(\epsilon_m^\alpha)^2 + E_l(\epsilon_l^\alpha)^2\right]$$

$$\sigma_{m,l}^\alpha = \frac{\partial \rho \psi^\alpha}{\partial \epsilon_{m,l}^\alpha} = (1-\omega^\alpha) E_{m,l} \epsilon_{m,l}^\alpha$$

$$\mathbb{C}_s^\alpha = (1-\omega^\alpha)\left[E_m(\boldsymbol{M}^\alpha \otimes \boldsymbol{M}^\alpha) + E_l(\boldsymbol{L}^\alpha \otimes \boldsymbol{L}^\alpha)\right]$$

# Disk simplification

(Kakarla et al., 2021;Kakarla, 2020; Park and Kim, 2003)

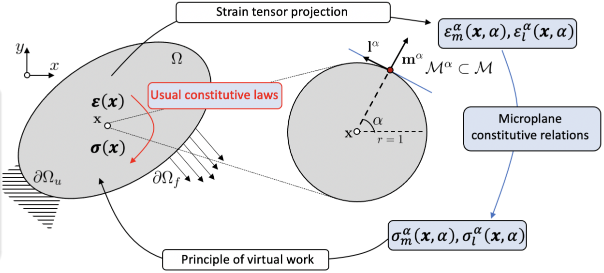


## Projection

$$\epsilon_m^\alpha = \boldsymbol{m}^\alpha \cdot \boldsymbol{\epsilon} \cdot \boldsymbol{m}^\alpha = \boldsymbol{M}^\alpha : \boldsymbol{\epsilon} = (\boldsymbol{m}^\alpha \otimes \boldsymbol{m}^\alpha) : \boldsymbol{\epsilon}$$

$$\epsilon_l^\alpha = \boldsymbol{l}^\alpha \cdot \boldsymbol{\epsilon} \cdot \boldsymbol{m}^\alpha = \boldsymbol{L}^\alpha : \boldsymbol{\epsilon} = (\boldsymbol{l}^\alpha \otimes \boldsymbol{m}^\alpha)^s : \boldsymbol{\epsilon}$$

## Principle of virtual work

$$\pi \boldsymbol{\sigma} : \delta \boldsymbol{\epsilon} = \int_{\mathcal{M}} (\sigma_m^\alpha \delta \epsilon_m^\alpha + \sigma_l^\alpha \delta \epsilon_l^\alpha) dS$$

$$\boldsymbol{\sigma} = \frac{2}{\pi} \sum_{N^\alpha} (\sigma_m^\alpha \boldsymbol{M}^\alpha + \sigma_l^\alpha \boldsymbol{L}^\alpha) W_\alpha$$

## Behaviour

$$\rho\psi^\alpha = (1-\omega^\alpha)/2 \left[ E_m (\epsilon_m^\alpha)^2 + E_l (\epsilon_l^\alpha)^2 \right]$$

$$\sigma_{m,l}^\alpha = \frac{\partial \rho \psi^\alpha}{\partial \epsilon_{m,l}^\alpha} = (1-\omega^\alpha) E_{m,l} \epsilon_{m,l}^\alpha$$

$$\mathbb{C}_s^\alpha = (1-\omega^\alpha) \left[ E_m (\boldsymbol{M}^\alpha \otimes \boldsymbol{M}^\alpha) + E_l (\boldsymbol{L}^\alpha \otimes \boldsymbol{L}^\alpha) \right]$$

# 2 CST example

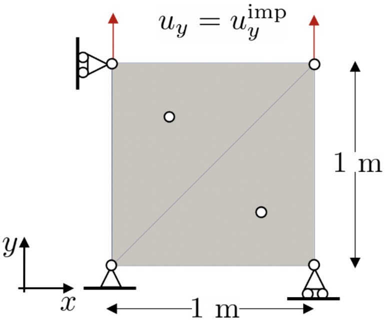


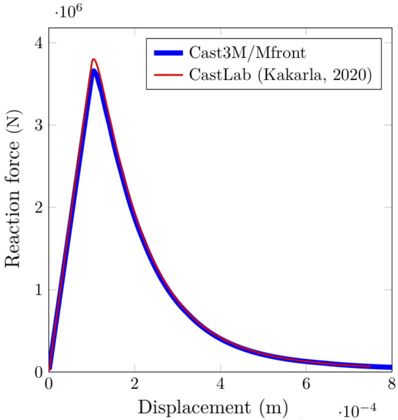


- 10 times faster than the results obtained by Kakarla et al., 2021, Kakarla, 2020

# Shi test

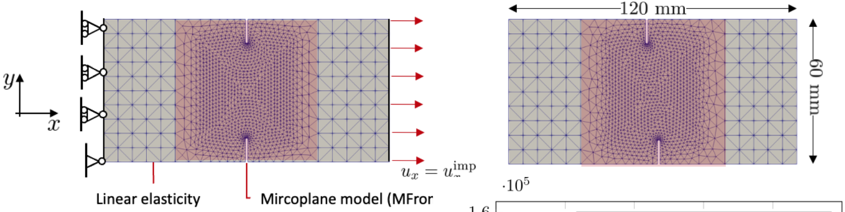
y
x
$u_x = u_x^{imp}$
Linear elasticity
Mircoplane model (MFror
120 mm
60 mm

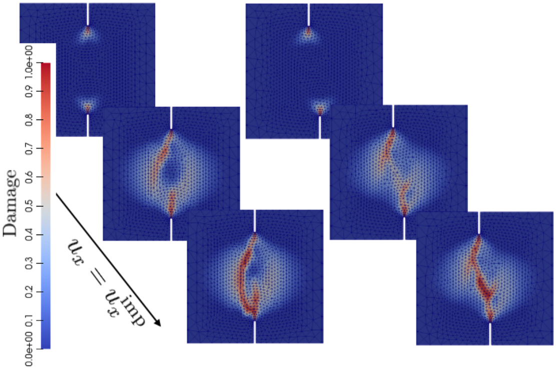
Damage
0.0e+00 0.1 0.2 0.3 0.4 0.5 0.6 0.7 0.8 0.9 1.0e+00
$u_x = u_x^{imp}$

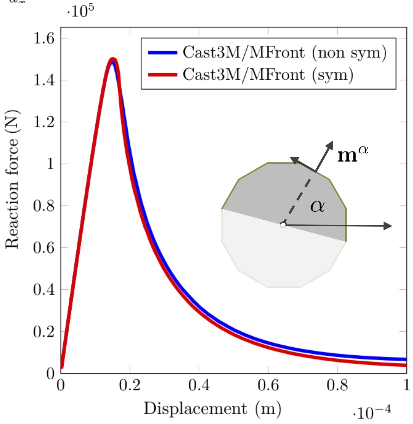
$\cdot 10^5$
Cast3M/MFront (non sym)
Cast3M/MFront (sym)
Reaction force (N)
Displacement (m)
$\cdot 10^{-4}$
$\mathbf{m}^\alpha$
$\alpha$

# Shi test: crack paths

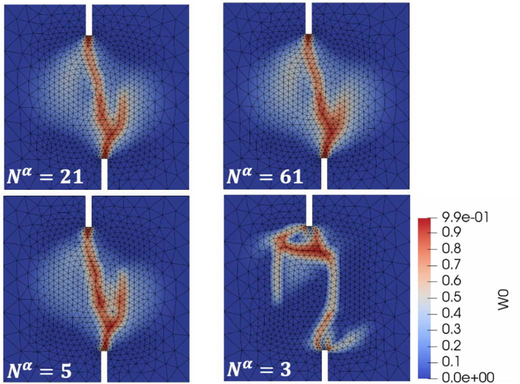


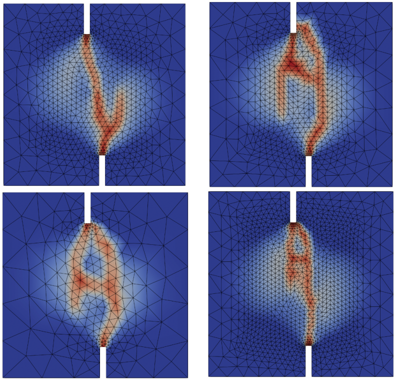

- Cracking convergence upon mesh refinement
- Energy regularization ⇒ different crack paths for different meshes

# Strong discontinuities
# E-FEM 2D

(e.g. Ortiz et al., 1987; Simo et al., 1993; Oliver, 1996; Oliver et al., 2004; Jirasek and Zimmermann, 2001; Simone et al., 2003)

# Kinematics

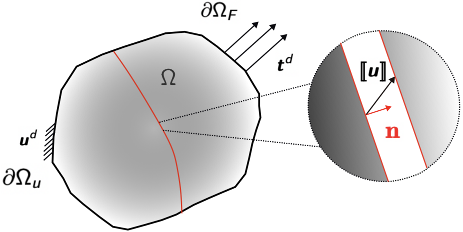


**Displacement field :**

$$\boldsymbol{u}(\boldsymbol{x},t) = \bar{\boldsymbol{u}}(\boldsymbol{x},t) + \mathcal{H}_\Gamma(\boldsymbol{x})[\![\boldsymbol{u}]\!](\boldsymbol{x},t)$$

**Strain field :**

$$\boldsymbol{\varepsilon} = \nabla^s\bar{\boldsymbol{u}}(\boldsymbol{x},t) + \mathcal{H}_\Gamma(\boldsymbol{x})\nabla^s[\![\boldsymbol{u}]\!](\boldsymbol{x},t) + \delta_\Gamma\left([\![\boldsymbol{u}]\!] \otimes \boldsymbol{n}\right)^s$$

**Hu-Washizu variational principle (weak formulation with three fields) :**

$$\int_\Omega \boldsymbol{\sigma} : \nabla^s\boldsymbol{u}^\star d\Omega + \int_\Omega \boldsymbol{\sigma}^\star : (\nabla^s\boldsymbol{u} - \boldsymbol{\varepsilon})\, d\Omega + \int_\Omega \boldsymbol{\varepsilon}^\star : (\tilde{\boldsymbol{\sigma}}(\boldsymbol{\varepsilon}) - \boldsymbol{\sigma}) = \int_{\partial\Omega_F} \boldsymbol{t}^d \cdot \boldsymbol{u}^\star dS$$

# Enrichment and numerical solutions

**Different approaches available (Jirásek, 2000) :** SOS, KOS and SKON

$$\boldsymbol{u} = \mathbf{N}\mathbf{d} + \mathbf{N}_c\mathbf{d}_c$$

$$\boldsymbol{\varepsilon} = \mathbf{B}\mathbf{d} + \mathbf{G}\mathbf{e}$$

$$\boldsymbol{\varepsilon}^\star = \mathbf{B}\mathbf{d}^\star + \mathbf{G}^\star\mathbf{e}^\star$$

$$\boldsymbol{\sigma} = \mathbf{S}\mathbf{s}$$

into the variational formulation

$$\Longrightarrow$$

$$\int_\Omega \mathbf{B}^{\mathrm{T}}\tilde{\boldsymbol{\sigma}}\left(\mathbf{B}\mathbf{d} + \mathbf{G}\mathbf{e}\right) d\Omega = \boldsymbol{f}_{\mathrm{ext}}$$

$$\int_\Omega \mathbf{G}^\star\tilde{\boldsymbol{\sigma}}\left(\mathbf{B}\mathbf{d} + \mathbf{G}\mathbf{e}\right) d\Omega = \mathbf{0}$$

$$\mathbf{G}^\star = \left(\delta_\Gamma - \frac{\mathrm{meas}(\Gamma_{\mathrm{e}})}{\mathrm{meas}(\Omega_{\mathrm{e}})}\right)\boldsymbol{\mathcal{N}}^{\mathrm{T}}$$

# Numerical solution (Alfaiate et al., 2002 for traction-separation law)

**Continuity of the traction vector for each element:**

$$\int_{\Omega_e} \left( \delta_\Gamma - \frac{\mathrm{meas}(\Gamma_\mathrm{e})}{\mathrm{meas}(\Omega_\mathrm{e})} \right) \boldsymbol{\mathcal{N}}^\mathrm{T} \tilde{\boldsymbol{\sigma}} d\Omega \quad \Rightarrow \boldsymbol{t}_\Gamma = \boldsymbol{\mathcal{N}}^\mathrm{T} \tilde{\boldsymbol{\sigma}} \quad \text{CST elements}$$

**Problem to solve:**

$$\mathbf{r}(\mathbf{d},\mathbf{e}) = \mathbf{f}_{\mathrm{int}}(\mathbf{d},\mathbf{e}) - \mathbf{f}_{\mathrm{ext}} = \mathbf{0}$$

$$\mathbf{h}^\mathrm{e}(\mathbf{d},\mathbf{e}) = \boldsymbol{\mathcal{N}}^\mathrm{T} \tilde{\boldsymbol{\sigma}}(\mathbf{d},\mathbf{e}) - \mathbf{t}_\Gamma(\mathbf{e}) = \mathbf{0} \quad \forall \Omega_e \in \mathrm{E}_{\mathrm{fiss}}$$

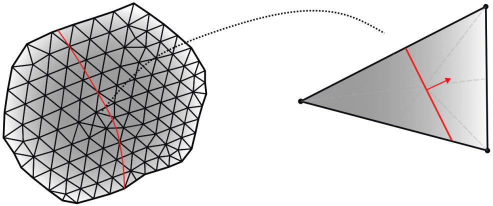

Equivalent to a non-linear behaviour law $\Longrightarrow$ Mfront
*(need to add matrix operations extensions...)*

# 1D bar response

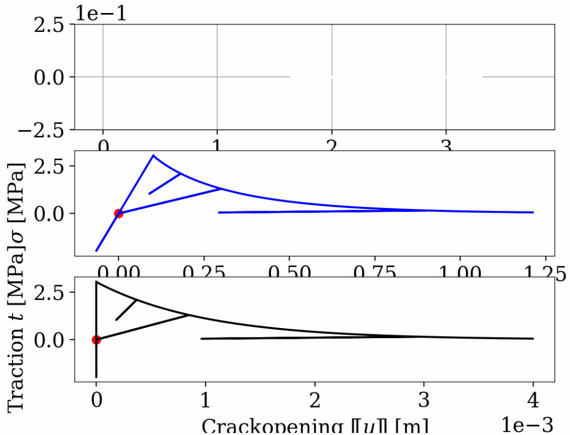

# Shi-test

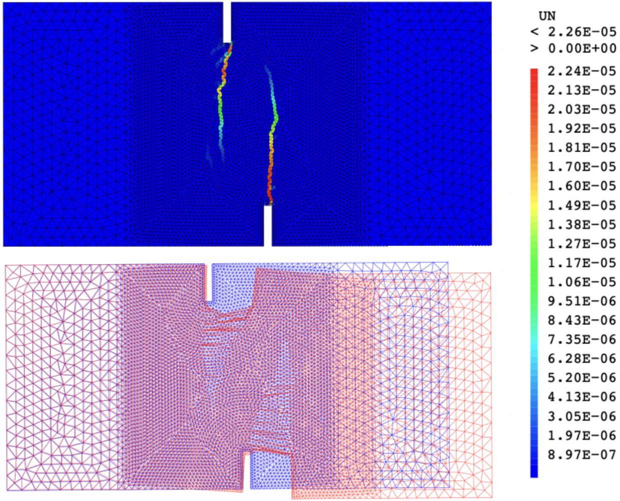
UN
< 2.26E-05
> 0.00E+00
2.24E-05
2.13E-05
2.03E-05
1.92E-05
1.81E-05
1.70E-05
1.60E-05
1.49E-05
1.38E-05
1.27E-05
1.17E-05
1.06E-05
9.51E-06
8.43E-06
7.35E-06
6.28E-06
5.20E-06
4.13E-06
3.05E-06
1.97E-06
8.97E-07

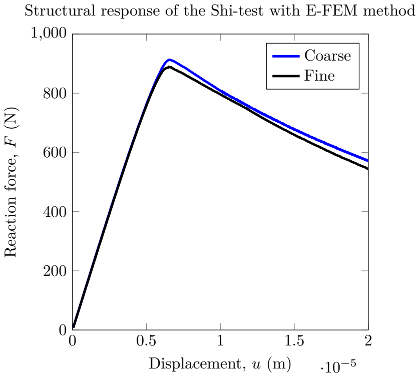
Structural response of the Shi-test with E-FEM method
Reaction force, $F$ (N)
1,000
800
600
400
200
0
Coarse
Fine
0
0.5
1
1.5
2
Displacement, $u$ (m)
$\cdot 10^{-5}$

# Shi-test

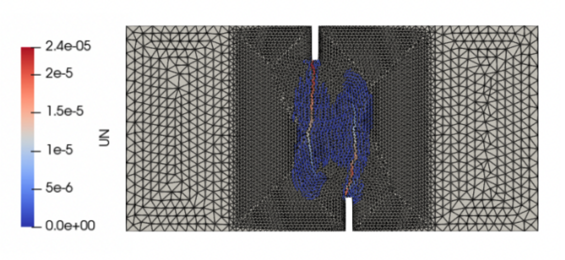


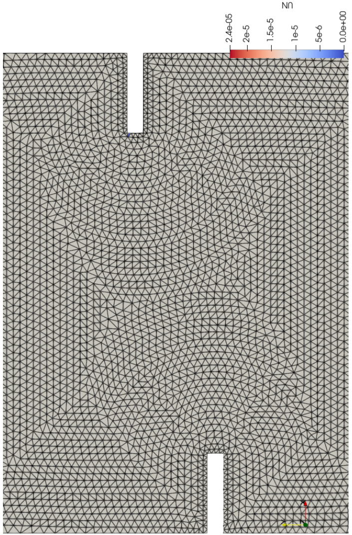

# 3-point bending

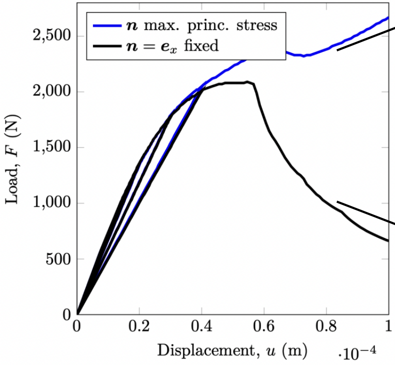


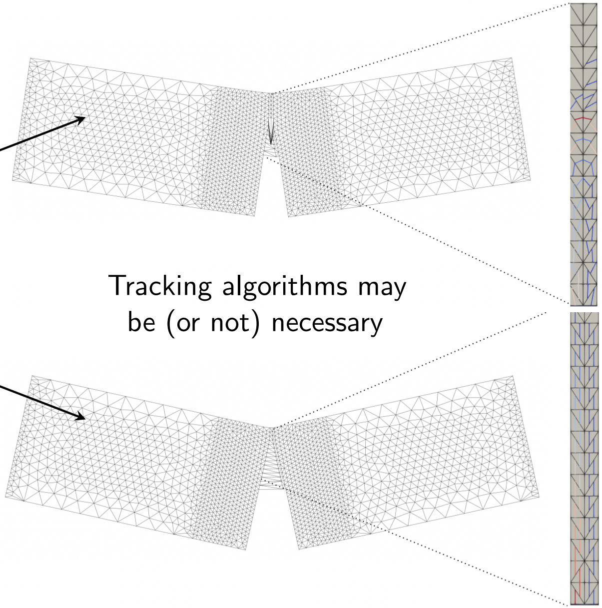

Tracking algorithms may be (or not) necessary

# Modelling of dissipative mechanisms for masonry-like materials

# Basic principles

- Homogenised material

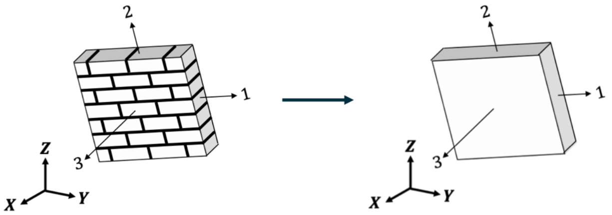


- Framework of the thermodynamics of irreversible processes

***Decomposition of the Gibbs free enthalpy density***

$$\rho\Psi^{\star} = \rho\Psi^{\star n}(\sigma_i, d_i) + \rho\Psi^{\star s}(\sigma_k, d_i, \sigma_k^{\pi}, \alpha_k), \quad (i,k) \in [\![1;3]\!] \times [\![4;6]\!]$$

Normal contribution Shear contribution

$\rightarrow$ coupling between orthotropic elasticity, damage and plasticity

# Modelled mechanisms: cracking to damage

- Damage evolution → mainly driven by cracks in mortar joints


Dais et al., 2021

## *Decomposition of the compliance tensor decomposition*

$$\mathbb{S}^{eff} = \mathbb{S}^0 + \Delta\mathbb{S} = \mathbb{S}^0 + \sum_{i=1,3} \left( d_i \ \mathbb{A}^{(i)} : \mathbb{S}^0 \right)$$

$d_i$ scalar damage variable

$\mathbb{A}^{(i)}$ damage effect tensor

$\mathbb{S}^0$ initial compliance tensor

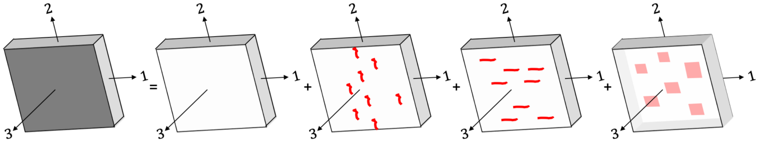


$$\mathbb{S}^{eff} = \mathbb{S}^0 + d_1\mathbb{A}^{(1)}:\mathbb{S}^0 + d_1\mathbb{A}^{(2)}:\mathbb{S}^0 + d_1\mathbb{A}^{(3)}:\mathbb{S}^0$$

*Crack families and effect on the compliance tensor*
Tisserand et al., 2022

# Modelled mechanisms: unilateral effect

- Seismic analyses involve alternating loading → crack closure

### *Normal stress partition into a positive and negative part*

based on Ladevèze, 1983

$$\sigma_i = \langle \sigma_i \rangle_+ + \langle \sigma_i \rangle_-, \quad i \in \{1,2,3\}$$

### *Coupling between orthotropic elasticity and damage for normal direction*

$$\rho \Psi^{\star n} = \frac{1}{2} \left[ (1 + d_i) \frac{\langle \sigma_i \rangle_+^2}{E_i} + \frac{\langle \sigma_i \rangle_-^2}{E_i} - 2 \frac{\nu_{il}}{E_i} \sigma_i \sigma_l - 2 \frac{\nu_{im}}{E_i} \sigma_i \sigma_m \right], \quad (i,l,m) = (1,2,3)$$

### *Normal strain*

$$\varepsilon_i = \rho \frac{\partial \Psi^{\star n}}{\partial \sigma_i} = (1 + d_i) \frac{\langle \sigma_i \rangle_+}{E_i} + \frac{\langle \sigma_i \rangle_-}{E_i} - \frac{\nu_{il}}{E_i} \sigma_l - \frac{\nu_{im}}{E_i} \sigma_m, \quad (i,l,m) = (1,2,3)$$

# Modelled mechanisms: internal sliding and friction

- Frictional sliding at crack surfaces $\rightarrow$ hysteretic dissipation and permanents strains

### *Coupling between friction and damage for shear direction*

based on Desmorat et al., 2007

$$\rho\Psi^{\star s} = \frac{1}{4G_{pq}}\left[\frac{\left(\sigma_k - \sigma_k^\pi\right)^2}{1 - g_k\left(d_p,d_q\right)} + \frac{\left(\sigma_k^\pi\right)^2}{g_k\left(d_p,d_q\right)} - w_k^s\right], \quad k(\leftrightarrow pq) \in [\![4;6]\!]$$

### *Shear stress*

$$\sigma_k = 2G_{pq}\left[1 - g_k\left(d_p,d_q\right)\right]\varepsilon_k + 2G_{pq}g_k\left(d_p,d_q\right)\left[\varepsilon_k - \varepsilon_k^\pi\right], \quad k(\leftrightarrow pq) \in [\![4;6]\!]$$

### *Threshold functions (frictional resistance and confinement effects)*

$$f_k = \left|\sigma_k^\pi - X_k\right| + \mu_k\left[\langle\sigma_p\rangle_- + \langle\sigma_q\rangle_-\right] \leq 0, \quad k(\leftrightarrow pq) \in [\![4;6]\!]$$

- Plastic flow develops independently along the orthotropic directions of masonry

# Validation: MTest

## Unidirectional traction/compression test

(damage + unilateral effect)

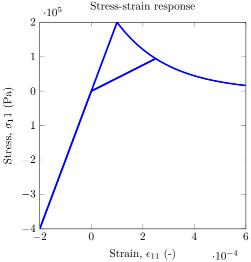


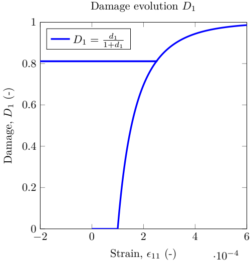


Unidirectional tensile/compressive test along direction 1
(left) Stress-strain response (right) Evolution of damage variable D1

## Cyclic shear test

(damage + friction)

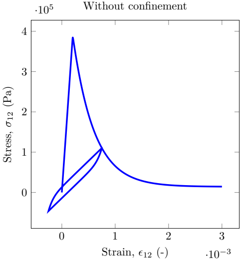


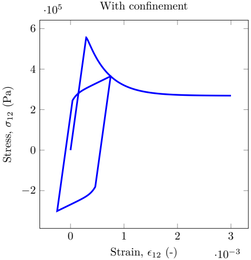


Stress-strain response for (left) Cyclic shear test without stress confinement (right) Cyclic shear test with stress confinement

# Example: Cyclic shear test

- Masonry panel under cyclic loading (Anthoine et al., 1995)

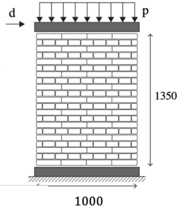


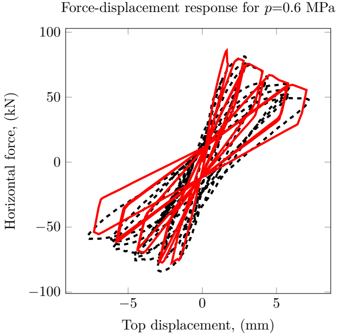


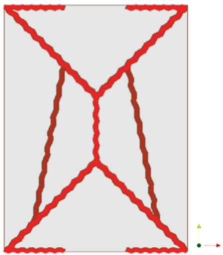

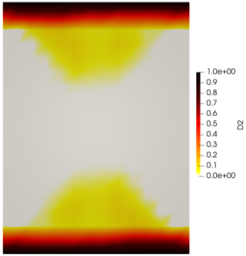


(left) Comparisons between experimental (black dashed line) and numerical (red solid line) force-displacement response curve under cyclic loading (middle) Experimental crack pattern (Anthoine et al., 1995) (right) Numerical damage map (Tisserand et al., 2022)

# Conclusion

# Conclusion

- **Work done**
  - Three different models implemented with Mfront
  - Additional matrix operations required in `TFELMathExtension.hxx` for E-FEM
- **Perspectives**
  - Couple formulations with **nonlocal** regularization
  - Extension to bars, plates and shells
  - Extension to **3D**: microplane and E-FEM

# Merci de votre attention

# References I


Alfaiate, J., G.N. Wells, and L.J. Sluys (Apr. 2002). "On the use of embedded discontinuity elements with crack path continuity for mode-I and mixed-mode fracture". en. In: *Engineering Fracture Mechanics* 69.6, pp. 661–686. ISSN: 00137944.

Anthoine, A, Georges Magonette, and Guido Magenes (1995). "Shear-compression testing and analysis of brick masonry walls". In: *Tenth European Conference on Earthquake Engineering* 3, pp. 1657–1662.

Bažant, Zdeněk P. and Pietro G. Gambarova (Sept. 1984). "Crack Shear in Concrete: Crack Band Microplane Model". In: *Journal of Structural Engineering* 110.9, pp. 2015–2035. ISSN: 0733-9445, 1943-541X. (Visited on 09/26/2020).

Bažant, Zdeněk P., Yuyin Xiang, and Pere C. Prat (Mar. 1996). "Microplane Model for Concrete. I: Stress-Strain Boundaries and Finite Strain". en. In: *Journal of Engineering Mechanics* 122.3, pp. 245–254. ISSN: 0733-9399, 1943-7889. (Visited on 09/26/2020).

Caner, F.C. and Z.P. Bažant (2013). "Microplane Model M7 for Plain Concrete. I: Formulation". In: *Journal of Engineering Mechanics* 139(12), pp. 1724–1735.

Dais, Dimitris, İhsan Engin Bal, Eleni Smyrou, and Vasilis Sarhosis (2021). "Automatic crack classification and segmentation on masonry surfaces using convolutional neural networks and transfer learning". In: *Automation in Construction* 125, p. 103606. ISSN: 0926-5805.

Desmorat, Rodrigue, F. Ragueneau, and H. Pham (2007). "Continuum damage mechanics for hysteresis and fatigue of quasi-brittle materials and structures". In: *International Journal for Numerical and Analytical Methods in Geomechanics* 31, pp. 307 –329. DOI: 10.1002/nag.532.

Huespe, Alfredo E. and Javier Oliver (2011). "Crack Models with Embedded Discontinuities". In: *Numerical Modeling of Concrete Cracking*. Ed. by Günter Hofstetter and Günther Meschke. Vienna: Springer Vienna, pp. 99–159. ISBN: 978-3-7091-0897-0. DOI: 10.1007/978-3-7091-0897-0_3. URL: https://doi.org/10.1007/978-3-7091-0897-0_3.

Jirasek, Milan and Thomas Zimmermann (2001). "Embedded crack model. Part II: combination with smeared cracks". In: *International Journal for Numerical Methods in Engineering* 50.6, pp. 1291–1305. ISSN: 0029-5981, 1097-0207.

# References II


Jirásek, Milan (2000). “Comparative study on F finite elements with embedded discontinuities”. In: *Comput. Methods Appl. Mech. Engrg.* 188, pp. 307–330.

Kakarla, S., G. Rastiello, B. Richard, and C. Giry (2021). “Coupled continuous–discrete formulation based on microplane and strong discontinuity models for representing non-orthogonal intersecting cracks”. In: *Engineering Fracture Mechanics* 245.

Kakarla, Santosh (2020). “From anisotropic damage to multiple cracks by coupling a microplane model and a strong discontinuity formulation in the Embedded Finite Element Method”. PhD thesis. Université Paris-Saclay - CEA - Service d’études mécaniques et thermiques - France. ENS Paris-Saclay.

Ladevèze, Pierre (1983). *Sur une théorie de l’endommagement anisotrope*. Laboratoire de Mécanique et Technologie.

Lemaitre, J. and R. Desmorat (2005). *Engineering Damage Mechanics: ductile, creep, fatigue and brittle failures.* Springer Nature Switzerland AG.

Oliver, J. (Nov. 1996). “Modelling strong discontinuities in solid mechanics via strain softening constitutive equations. Part 1: fundamentals”. en. In: *International Journal for Numerical Methods in Engineering* 39.21, pp. 3575–3600. ISSN: 0029-5981, 1097-0207. DOI: 10.1002/(SICI)1097-0207(19961115)39:21<3575::AID-NME65>3.0.CO;2-E. URL: https://onlinelibrary.wiley.com/doi/10.1002/(SICI)1097-0207(19961115)39:21<3575::AID-NME65>3.0.CO;2-E (visited on 07/08/2022).

Oliver, J., A. Huespe, M.D.G. Pulido, and S. Blanco (Feb. 2004). “Computational modeling of cracking of concrete in strong discontinuity settings”. en. In: *Computers and Concrete* 1.1, pp. 61–76. DOI: 10.12989/CAC.2004.1.1.061. URL: https://doi.org/10.12989/CAC.2004.1.1.061 (visited on 02/18/2022).

# References III


Ortiz, Michael, Yves Leroy, and Alan Needleman (Mar. 1987). "A finite element method for localized failure analysis". en. In: *Computer Methods in Applied Mechanics and Engineering* 61.2, pp. 189–214. ISSN: 00457825. DOI: 10.1016/0045-7825(87)90004-1. URL: https://linkinghub.elsevier.com/retrieve/pii/0045782587900041 (visited on 07/08/2022).

Park, Honggun and Hakjun Kim (Mar. 2003). "Microplane Model for Reinforced-Concrete Planar Members in Tension-Compression". en. In: *Journal of Structural Engineering* 129.3, pp. 337–345. ISSN: 0733-9445, 1943-541X. (Visited on 09/28/2020).

Simo, J. C., J. Oliver, and F. Armero (1993). "An analysis of strong discontinuities induced by strain-softening in rate-independent inelastic solids". en. In: *Computational Mechanics* 12.5, pp. 277–296. ISSN: 0178-7675, 1432-0924. DOI: 10.1007/BF00372173. URL: http://link.springer.com/10.1007/BF00372173 (visited on 07/08/2022).

Simone, Angelo, Garth N. Wells, and Lambertus J. Sluys (2003). "From continuous to discontinuous failure in a gradient-enhanced continuum damage model". In: *Computer Methods in Applied Mechanics and Engineering* 192.41-42, pp. 4581–4607. ISSN: 00457825.

Taylor, G. I. (1938). "Plastic strain in metals". In: *J. Inst. Metals* 62, pp. 307–324.

Tisserand, Pierre-Jean, Héloïse Rostagni, Cédric Giry, Thi Thanh Huyen Nguyen, Rodrigue Desmorat, and Frédéric Ragueneau (2022). "An orthotropic damage model with internal sliding and friction for masonry-like material". In: *Engineering Fracture Mechanics* 267, p. 108397. ISSN: 0013-7944.